

A STABLE CLOCK ERROR MODEL USING COUPLED FIRST- AND SECOND-ORDER GAUSS-MARKOV PROCESSES

Russell Carpenter* and Taesul Lee†

Long data outages may occur in applications of global navigation satellite system technology to orbit determination for missions that spend significant fractions of their orbits above the navigation satellite constellation(s). Current clock error models based on the random walk idealization may not be suitable in these circumstances, since the covariance of the clock errors may become large enough to overflow flight computer arithmetic. A model that is stable, but which approximates the existing models over short time horizons is desirable. A coupled first- and second-order Gauss-Markov process is such a model.

INTRODUCTION

According to Van Dierendonck,¹ the Allan variance technique represents the power spectral density, $S(f)$, of a clock's frequency fluctuation as a function of frequency by

$$S(f) = h_2 f^2 + h_1 f + h_0 + h_{-1} f^{-1} + h_{-2} f^{-2} \quad (1)$$

where h_2 is the “white phase noise,” h_1 is the “flicker phase noise,” h_0 is the “white frequency noise,” h_{-1} is the “flicker frequency noise,” and h_{-2} is the “random walk frequency noise.” The random walk model developed in Brown and Hwang² makes use of the frequency noise terms only, i.e. h_0 , h_{-1} , and h_{-2} . These terms give rise to asymptotes on an Allan variance plot, an example of which Figure 1 shows. The white frequency noise asymptote is $\sqrt{h_0/2\tau}$, and dominates at small averaging times. The flicker frequency noise asymptote is $\sqrt{(2 \ln 2)h_{-1}}$, and dominates at intermediate averaging times. The random walk frequency noise asymptote is $2\pi\sqrt{h_{-2}\tau/6}$, and dominates at larger averaging times. Figure 1 also shows the Allan variance of the random walk model developed in Ref. 2, and the Allan variance of a Gauss-Markov model, discussed below (the appendix of this work specifies the random walk model).

As Figure 1 shows, the random walk model nicely approximates the asymptotic Allan variance plot over all time scales, while avoiding certain model representation

*Flight Dynamics Analysis Branch, NASA Goddard Space Flight Center, Code 595, Greenbelt, MD 20771.

†a.i. solutions, Inc., 10001 Dereewood Lane, Suite 215, Lanham, MD 20706.

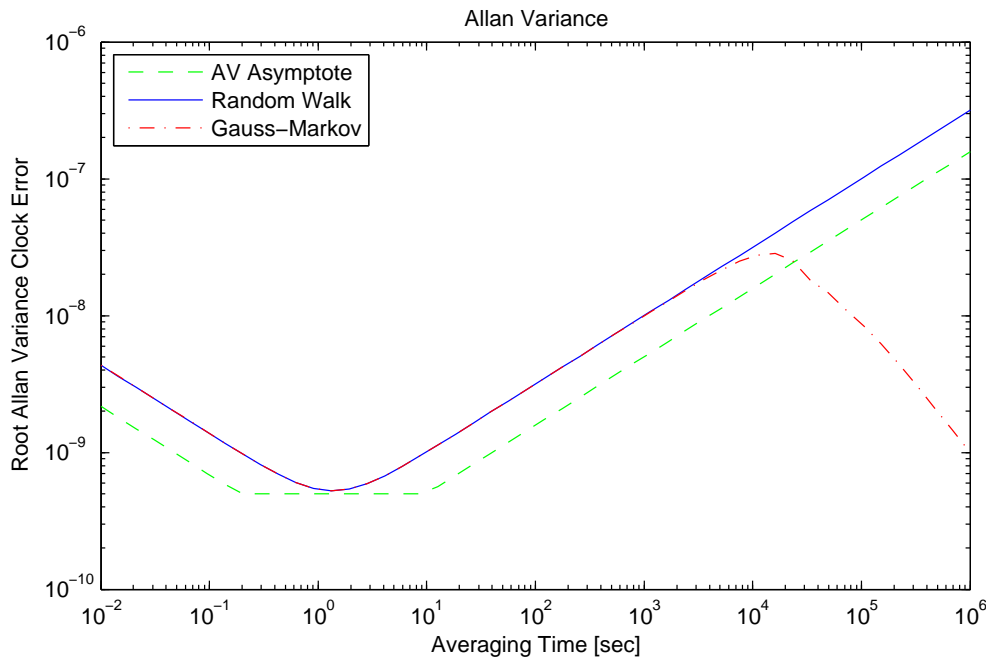


Figure 1 The Gauss-Markov model closely approximates the Allan variance of the random walk model over a wide range of sample times.

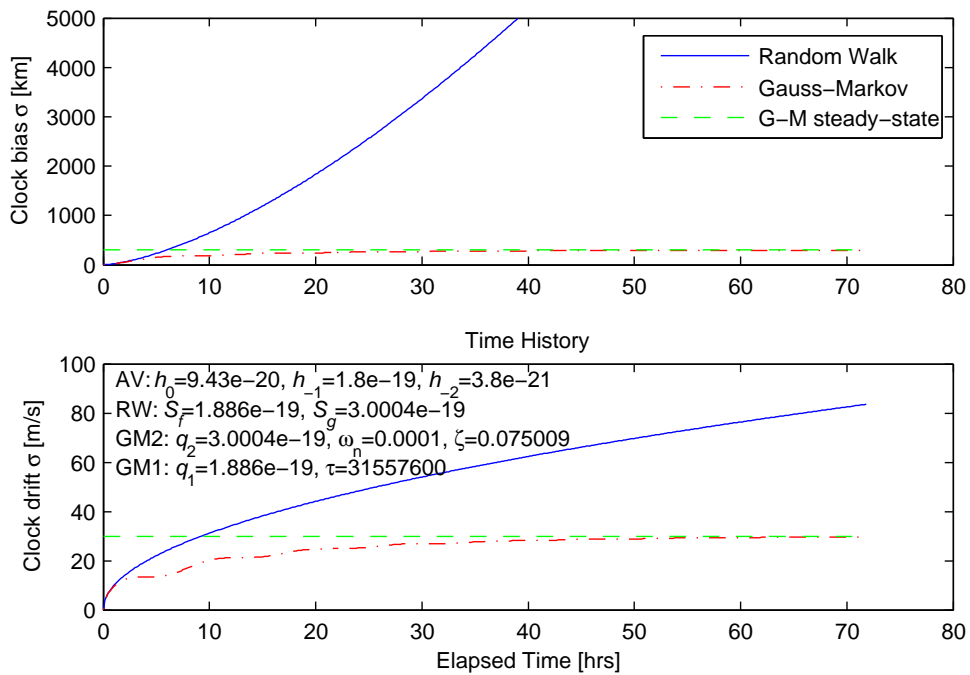


Figure 2 The random walk model is unstable; the Gauss-Markov model is stable.

issues related to the flicker frequency noise.² The possible difficulty with this model is evident in Figure 2, i.e. the clock bias error envelope becomes larger than the diameter of the earth within two days. Nominally, global navigation satellite system receivers process measurements from four or more satellites at intervals on the order of seconds, so the error growth Figure 2 shows does not occur. However, in a medium, highly-elliptical, or geosynchronous Earth orbit mission, even nominal satellite visibility conditions may not permit rectification of the time bias estimate for long periods of time. Allowing the uncertainty to continue to grow as Figure 2 shows appears harmless enough, since a Kalman filter should be able to quickly re-converge to reasonable uncertainty levels once visibility conditions permit additional measurement processing. In fact, a very large covariance is somewhat desirable in such cases, if the filter has a residual edit function that could be triggered by large residuals that might occur at measurement re-acquisition.

As stated at the outset, the desirability of this approach will be negated if the covariance becomes large enough to overflow the flight computer's arithmetic, causing the filter software to crash. Figure 2 indicates that, for the somewhat average clock parameters simulated here, this condition probably would not occur for several days. (This statement assumes the use a $U - D$ factorized filter, which stores quantities related to the square root of the covariance; this problem would be accentuated in a filter storing the total covariance matrix.) Since the random walk model is much simpler than the Gauss-Markov model, in most cases it may be adequate.

If on the other hand a requirement exists for a filter to operate through very long outages, or if a filter is tuned or mechanized in such a way as to create the possibility of covariance overflow, a coupled first- and second-order Gauss-Markov model proposed herein may be used. As Figures 1 – 3 show, the model is stable, reaching a specified steady-state value after a few hours, and it closely approximates both the time histories and the Allan variances of the random walk model over shorter time intervals. Note that we do not mean to imply that real clocks have bounded error growth; we merely suggest that open-loop-stable error models may be more suitable for navigation filters in some applications.

PROBLEM STATEMENT AND SOLUTION

The Gauss-Markov clock bias model proposed herein is a coupling of a first-order Gauss-Markov (FOGM) process driving the bias state directly, and a second-order Gauss-Markov (SOGM) process driving the bias state via integration of its direct effect on the clock drift. Let b represent the clock bias, and d represent the clock drift. Then, the continuous-time representation of the model is

$$\begin{bmatrix} \dot{b}(t) \\ \dot{d}(t) \end{bmatrix} = \begin{bmatrix} -1/\tau & 1 \\ -\omega_n^2 & -2\zeta\omega_n \end{bmatrix} \begin{bmatrix} b(t) \\ d(t) \end{bmatrix} + \begin{bmatrix} w_1(t) \\ w_2(t) \end{bmatrix} \quad (2)$$

where τ is the FOGM time constant, w_1 is the FOGM zero-mean driving white noise with power spectral density (PSD) q_1 , ω_n is the SOGM natural frequency, ζ is the

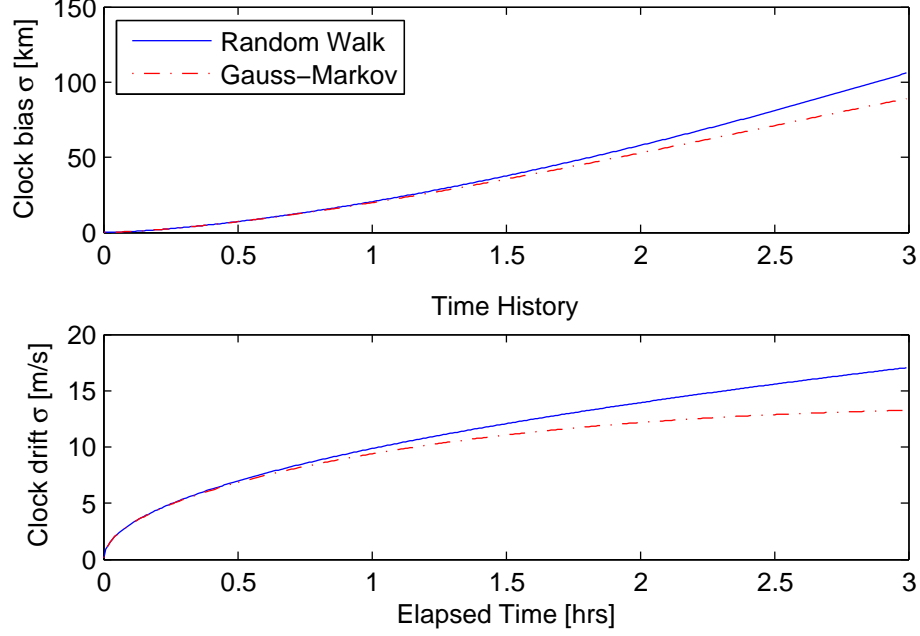


Figure 3 Over short intervals, the Gauss-Markov and random walk models agree well.

SOGM damping ratio, and w_2 is the SOGM zero-mean driving white noise with PSD q_2 . Note that the SOGM is not merely an integrated FOGM; as the appendix shows, the latter is not stable.

Although Eq. 2 is a stochastic differential equation, we can seek a mean-square solution. With $x = [b, d]'$ and $w = [w_1, w_2]'$, Eq. 2 becomes:

$$\dot{x}(t) = Ax(t) + w(t) \quad (3)$$

where A is given by

$$A = \begin{bmatrix} -1/\tau & 1 \\ -\omega_n^2 & -2\zeta\omega_n \end{bmatrix}. \quad (4)$$

Since $E[w] = 0$, the mean solution, $\bar{x}(t)$, will be given by the homogeneous solution of Eq. 2. The covariance, $P = E[(x - \bar{x})(x - \bar{x})']$, where

$$P = \begin{bmatrix} p_{11} & p_{12} \\ p_{21} & p_{22} \end{bmatrix} = \begin{bmatrix} p_{bb} & p_{bd} \\ p_{bd} & p_{dd} \end{bmatrix} \quad (5)$$

must satisfy

$$\dot{P}(t) = AP(t) + P(t)A' + Q, \quad (6)$$

where $Q = \text{diag}(q_1, q_2)$.

Analytical Solution

Let us first find the homogeneous solution for Eq. 2, in the form:

$$x(t) = \Phi(t, t_o)x(t_o). \quad (7)$$

The state transition function $\Phi(t, t_o)$ must possess the following properties:

$$\dot{\Phi}(t, t_o) = A\Phi(t, t_o), \quad \Phi(t_o, t_o) = I \quad (8)$$

$$\Phi(t, t_o) = \Phi(t, t_1)\Phi(t_1, t_o), \quad t_o < t_1 < t \quad (9)$$

$$\Phi(t, t_o) = \Phi(\Delta t), \quad \Delta t = t - t_o \quad (10)$$

A state transition function that satisfies these properties is the following:

$$\Phi(\Delta t) = \frac{e^{a\Delta t}}{b} \begin{bmatrix} b \cos b\Delta t + (a + 2\zeta\omega_n) \sin b\Delta t & \sin b\Delta t \\ -\omega_n^2 \sin b\Delta t & b \cos b\Delta t + (a + \beta) \sin b\Delta t \end{bmatrix} \quad (11)$$

where

$$\beta = 1/\tau, \quad (12)$$

$$a = -\frac{1}{2}(\beta + 2\zeta\omega_n), \quad (13)$$

$$b = \sqrt{\omega_d^2 + \beta\zeta\omega_n - \frac{1}{4}\beta^2}, \quad (14)$$

$$\omega_d = \omega_n\sqrt{1 - \zeta^2}, \quad (15)$$

and we assume that $b^2 > 0$. Since the noise input is zero-mean, this state transition matrix allows one to find the mean solution, $\bar{x}(t)$, to Eq. 2.

Let

$$c = -\frac{\beta}{2} + \zeta\omega_n;$$

then, the covariance is given by the following:

$$p_{11}(\Delta t) = q_1 \left[\frac{e^{2a\Delta t} - 1}{4a} \left(1 + \frac{c^2}{b^2} \right) + \frac{e^{2a\Delta t} \sin 2b\Delta t}{4(a^2 + b^2)} \left(\frac{b^2 - c^2 + 2ac}{b} \right) + \frac{e^{2a\Delta t} \cos 2b\Delta t - 1}{4(a^2 + b^2)} \left(\frac{ab^2 - ac^2 + 2b^2c}{b^2} \right) \right] \quad (16)$$

$$p_{22}(\Delta t) = q_2 \left[\frac{e^{2a\Delta t} - 1}{4a} \left(1 + \frac{c^2}{b^2} \right) + \frac{e^{2a\Delta t} \sin 2b\Delta t}{4(a^2 + b^2)} \left(\frac{b^2 - c^2 + 2ac}{b} \right) + \frac{e^{2a\Delta t} \cos 2b\Delta t - 1}{4(a^2 + b^2)} \left(\frac{ab^2 - ac^2 + 2b^2c}{b^2} \right) \right] + \frac{q_2}{b^2} \left(\frac{e^{2a\Delta t} - 1}{4a} - \frac{e^{2a\Delta t}(b \sin 2b\Delta t + a \cos 2b\Delta t) - a}{4(a^2 + b^2)} \right) \quad (17)$$

$$p_{12}(\Delta t) = \frac{q_1 \omega_n^2}{b^2} \left[\frac{c}{4a} (1 - e^{2a\Delta t}) + \frac{e^{2a\Delta t} [(bc - ab) \sin 2b\Delta t + (ac - b^2) \cos 2b\Delta t] - (ac - b^2)}{4(a^2 + b^2)} \right] + \frac{q_2}{b^2} \left[\frac{c}{4a} (1 - e^{2a\Delta t}) + \frac{e^{2a\Delta t} [(ab + bc) \sin 2b\Delta t + (ac - b^2) \cos 2b\Delta t] - (ac - b^2)}{4(a^2 + b^2)} \right]. \quad (18)$$

Approximate Solution

In online filtering applications, the analytical solution may prove cumbersome to implement, and additionally, the time step may be small in comparison to the modes of the system. In such cases, an approximate solution may prove useful. The formal solution to Eq. 2 is

$$P(t + \Delta t) = \Phi(\Delta t)P(t)\Phi'(\Delta t) + S(\Delta t), \quad (19)$$

where

$$S(\Delta t) = \int_t^{t+\Delta t} \Phi(\tau)Q\Phi'(\tau)d\tau, \quad (20)$$

the simplest approximation to which is $S(\Delta t) = Q\Delta t$.

DISCUSSION

Characteristics of the Solution

Examining the solution given above, we see that the parameter a governs the rate of decay of all of the exponential terms. Therefore, we define the ‘‘rise time’’ as that interval within which the transient response of the covariance will reach a close approximation to the above steady-state value; thus, we define the rise time as follows:

$$t_r = -\frac{3}{a}. \quad (21)$$

Next, we note that all of the trigonometric terms are modulated by $2b$; thus we may view this value as a characteristic damped frequency of the coupled system. The period of the oscillation, Π , is then

$$\Pi = \pi/b \quad (22)$$

In the limit as $t \rightarrow \infty$, all the exponential terms in the analytical solution die out, so that the steady-state value of the covariance simplifies to:

$$P(\infty) = -\frac{1}{4a(a^2 + b^2)} \begin{bmatrix} q_2 + (2a^2 + b^2 + c^2 - 2ac)q_1 & \beta(q_2 + q_1\omega_n^2) \\ \beta(q_2 + q_1\omega_n^2) & (2a^2 + b^2 + c^2 + 2ac)q_2 + q_1\omega_n^4 \end{bmatrix} \quad (23)$$

Comparison of Numerical, Analytical, and Approximate Solutions

Figure 4 compares the approximate numerical and the exact analytical solutions for the time evolution of the covariances, for a particular set of parameters. Initially, the position error is a few percent, but it quickly decreases to a tiny fraction of a percent. The velocity error is never more than a fraction of a percent. In this example, the period of the oscillatory response, Π , is about 8.7 hours.

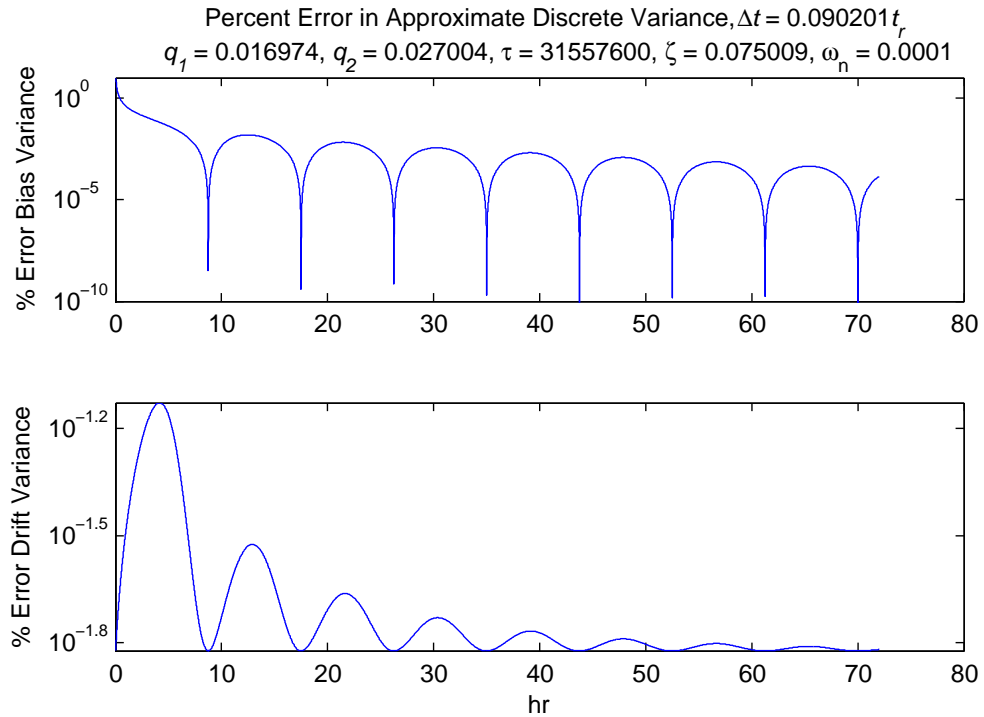


Figure 4 The approximate analytical solution agrees well with the exact solution.

Parameter Sensitivity

Figure 5 shows the results of a sensitivity analysis. The left and right columns show the sensitivity of the formal error in bias and drift, respectively, to parameter variations. The FOGM time constant varies from half a day to over a year, the SOGM damping varies from a very underdamped value of 10^{-5} to critical, and we varied the SOGM natural frequency so as to cover a similar range of bias and drift values to the ranges the other parameter variations produced. It is notable that varying ω_n produces a somewhat wider range of variability in bias than it does in drift, relative to the ranges of variation that the other parameters produce. This is similar to the relationship between bias and drift error that would result from a purely SOGM model, $\sigma_a/\sigma_b = \omega_n$, which the appendix shows. For this reason, we find that ω_n is a useful parameter for adjusting the relative magnitudes of bias and drift in steady-state, as the discussion below describes further.

Tuning

To use the coupled FOGM/SOGM process as a clock model, we wish to tune it such that it approximates the usual RW model over time intervals associated with filtering. For a FOGM, choosing the time constant, $\tau = 1/\beta$, to be much larger than the sampling interval causes the FOGM to resemble a RW over intervals less than the time constant. A similar effect occurs for a SOGM, by choosing the product $\zeta\omega_n$ much smaller than the sample interval. The corresponding parameter for the coupled FOGM/SOGM process is $1/a$ (recall that $a = -\beta/2 - \zeta\omega_n$); choosing $1/a$ to be much larger than the sampling interval will cause the coupled FOGM/SOGM process to resemble a RW over intervals shorter than $1/a$. It may also be desirable to select a value of ζ near unity so as to minimize any ringing that otherwise might creep into the coupled model from the SOGM dynamics; however, we have not found this to be a significant problem for even very underdamped values, as the sensitivity analysis described above shows.

Next, we wish for the slopes of the covariances of the coupled model to be similar to the RW model. The slopes for the coupled model are given by

$$\dot{p}_{22}(t) = q_2 - 2\omega_n^2 p_{12}(t) - 4\zeta\omega_n p_{22}(t) \quad (24)$$

$$\dot{p}_{12}(t) = p_{22}(t) - (\beta + 2\zeta\omega_n)p_{12}(t) - \omega_n^2 p_{11}(t) \quad (25)$$

$$\dot{p}_{11}(t) = 2p_{12}(t) + q_1 - 2\beta p_{11}(t) \quad (26)$$

whereas for the RW clock model, the slopes are given by

$$\dot{p}_{22} = q_2 \quad (27)$$

$$\dot{p}_{12}(t) = p_{22}(t) = q_2 t \quad (28)$$

$$\dot{p}_{11}(t) = 2p_{12}(t) + q_1 = q_2 t^2 + q_1 \quad (29)$$

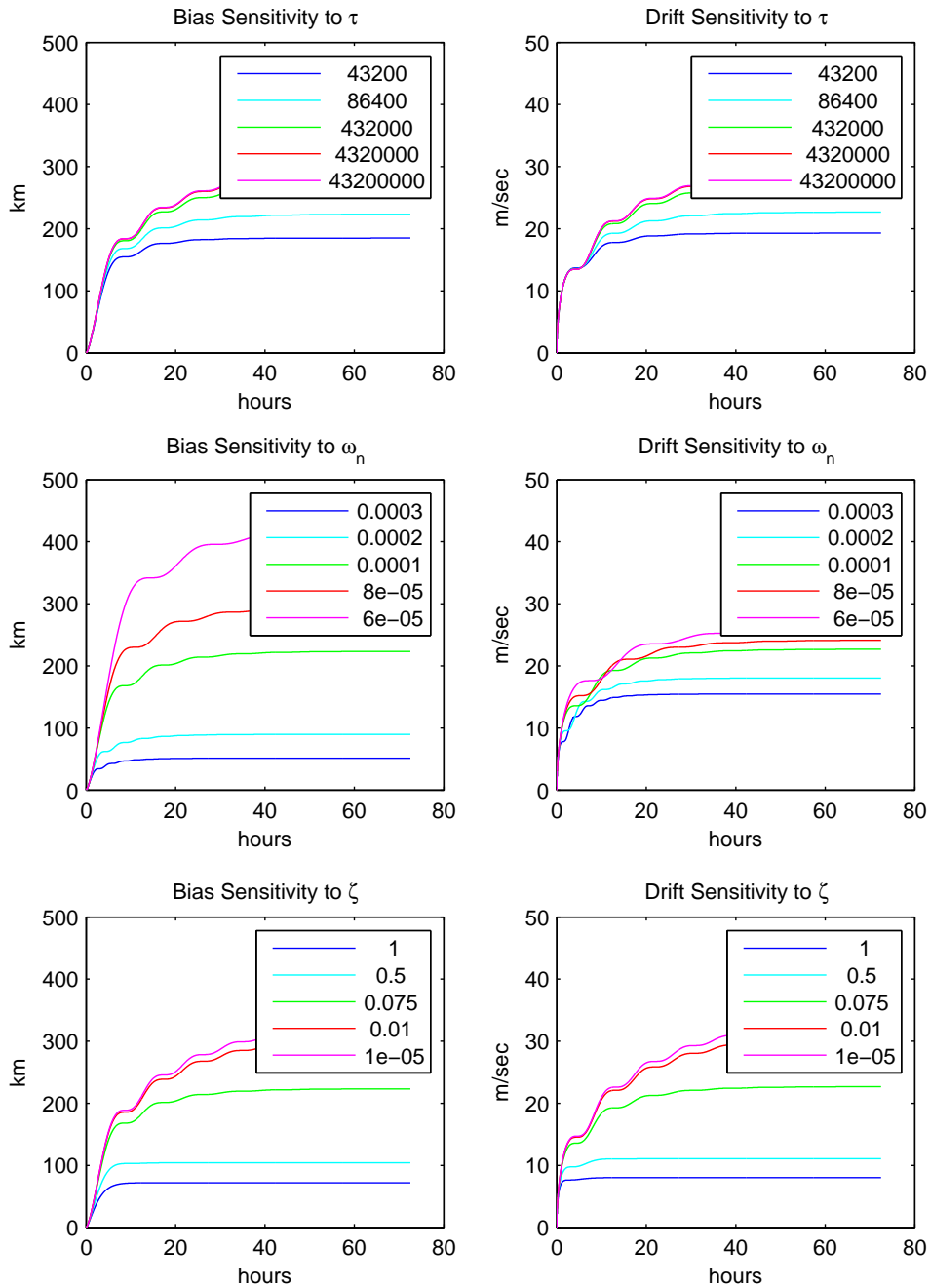


Figure 5 Sensitivity of formal error to parameter variations around baseline of $\tau = 86400$ sec, $\omega_n = 0.0001$ rad/sec, $\zeta = 0.075009$, $q_1 = 0.017$ m²/sec, $q_2 = 0.027$ m²/sec³.

Given that β and $\zeta\omega_n$ have been chosen to be small*, we can make the slopes approximately equal over time intervals less than $1/a$ by choosing q_1 and q_2 to be the same as in the RW model.

The final step in tuning the coupled model is to check the steady-state values to ensure the magnitudes are acceptable. We have found that adjustment of ω_n is an effective means for modulating the relative size of the steady-state drift versus the steady-state bias variance.

Ensembles of Sample Realizations

Figures 6 and 7 show a couple of examples of ensembles of sample realizations for two different parameter selections. These examples use the same process noise PSDs, but different values of the FOGM/SOGM parameters. Both use rather underdamped values of ζ . The product $\zeta\omega_n$ is of the same order in both examples however. The FOGM time constant is almost an order of magnitude larger, and ω_n is an order of magnitude larger, in Fig. 6. In both cases, the rise time is about 30 hours. The most notable difference between the two examples is the behavior of the sample realizations of the bias error, with the bias ensemble in Fig. 7 appearing less noise-like, which may or may not be of interest to filter performance.

CONCLUSION

The coupled first- and second-order Gauss-Markov model for clock errors which this work contributes may prove useful in a variety of applications. The model is open-loop stable, which means the designer of a navigation filter may definitively specify a maximum value for the magnitude of the error growth in the absence of measurements, thereby alleviating non-sensical results and numerical overflow issues. The model closely approximates a random walk over a designated rise time, so that over a given time interval of interest, the model may be tuned to match the error characteristics of real clocks whose random errors are adequately modeled by the Allan variance characteristics described in Refs. 1 and 2. If the analytical solution is not suitable for implementation in some cases, a remarkably simple approximation for the process noise covariance contribution over small time steps has shown to be adequate.

REFERENCES

- [1] A. J. v. Dierendonck, J. B. McGraw, and R. G. Brown, "Relationship Between Allan Variances and Kalman Filter Parameters," *Proceedings of the 16th Annual Precise Time and Time Interval (PTTI) Applications and Planning Meeting*, NASA Goddard Space Flight Center, November 1984, pp. 273–293.

*Since ζ is on the order of 1, then terms multiplied by ω_n^2 may also be neglected.

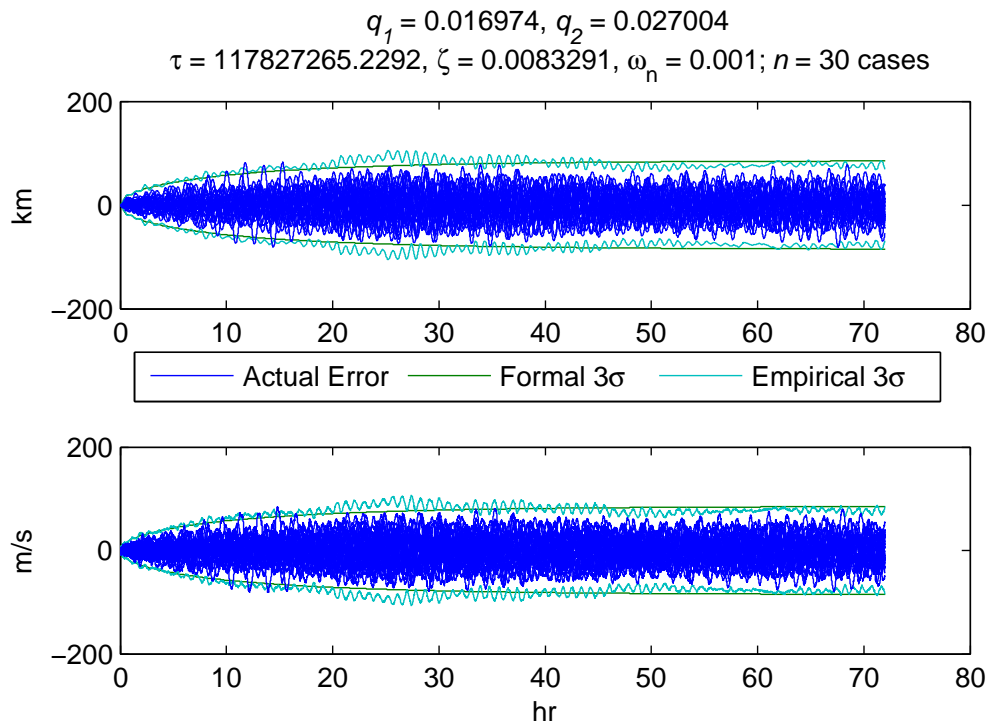


Figure 6 Sample Realization 1.

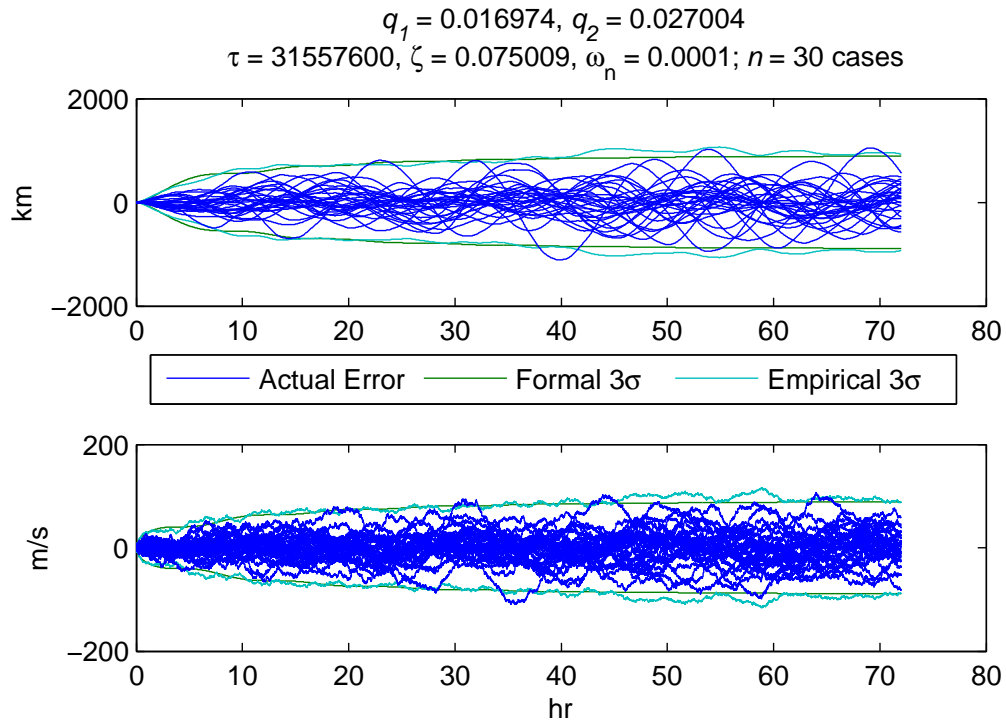


Figure 7 Sample Realization 2.

- [2] R. G. Brown and P. Y. Hwang, *Introduction to Random Signals and Applied Kalman Filtering*. New York, NY: John Wiley and Sons, Inc., 3rd ed., 1997.
- [3] M. C. Wang and G. E. Uhlenbeck, “On the Theory of Brownian Motion II,” *Selected Papers on Noise and Stochastic Processes* (N. Wax, ed.), pp. 113–132, Dover, 1954.

APPENDIX

Here, we specify the random walk, integrated first-order Gauss-Markov, and second-order Gauss-Markov models.

Random Walk Model

The random walk clock model of Ref. 2 is given by

$$\begin{bmatrix} \dot{b}(t) \\ \dot{d}(t) \end{bmatrix} = \begin{bmatrix} 0 & 1 \\ 0 & 0 \end{bmatrix} \begin{bmatrix} b(t) \\ d(t) \end{bmatrix} + \begin{bmatrix} w_1(t) \\ w_2(t) \end{bmatrix}, \quad (30)$$

which leads to the following state transition matrix,

$$\Phi(\Delta t) = \begin{bmatrix} 1 & \Delta t \\ 0 & 1 \end{bmatrix}, \quad (31)$$

and process noise covariance,

$$S(\Delta t) = \begin{bmatrix} q_1 \Delta t + q_2 \frac{\Delta t^3}{3} & q_2 \frac{\Delta t^2}{2} \\ q_2 \frac{\Delta t^2}{2} & q_2 \Delta t \end{bmatrix}. \quad (32)$$

Clearly, the clock drift variance increases linearly with elapsed time, and the clock bias increases as the cube of elapsed time.

Integrated First-Order Gauss-Markov Model

The integrated first-order Gauss-Markov model is given by

$$\begin{bmatrix} \dot{b}(t) \\ \dot{d}(t) \end{bmatrix} = \begin{bmatrix} 0 & 1 \\ 0 & -1/\tau \end{bmatrix} \begin{bmatrix} b(t) \\ d(t) \end{bmatrix} + \begin{bmatrix} 0 \\ w_2(t) \end{bmatrix}, \quad (33)$$

which leads to the following state transition matrix,

$$\Phi(\Delta t) = \begin{bmatrix} 1 & \tau (1 - e^{-\Delta t/\tau}) \\ 0 & e^{-\Delta t/\tau} \end{bmatrix}, \quad (34)$$

and process noise covariance,

$$S(\Delta t) = \frac{q_2 \tau}{2} \begin{bmatrix} \tau^2 \left\{ (1 - e^{-2\Delta t/\tau})^2 + \frac{2\Delta t}{\tau} + 4(1 - e^{-\Delta t/\tau}) \right\} & \tau (1 - e^{-\Delta t/\tau})^2 \\ \tau (1 - e^{-\Delta t/\tau})^2 & (1 - e^{-2\Delta t/\tau}) \end{bmatrix}. \quad (35)$$

Clearly, this is an unstable model, as the clock bias variance increases linearly with elapsed time.

Second-Order Gauss-Markov Process

The second-order Gauss-Markov model is given by

$$\begin{bmatrix} \dot{b}(t) \\ \dot{d}(t) \end{bmatrix} = \begin{bmatrix} 0 & 1 \\ -\omega_n^2 & -2\zeta\omega_n \end{bmatrix} \begin{bmatrix} b(t) \\ d(t) \end{bmatrix} + \begin{bmatrix} 0 \\ w_2(t) \end{bmatrix} \quad (36)$$

Reference 3 gives the following solution for the second-order Gauss-Markov process.

$$E[b(t)] = b_o \frac{e^{-\zeta\omega_n t}}{w_d} (\omega_d \cos \omega_d t + \zeta\omega_n \sin \omega_d t) + d_o \frac{e^{-\zeta\omega_n t}}{w_d} \sin \omega_d t \quad (37)$$

$$E[d(t)] = -b_o \omega_n^2 \frac{e^{-\zeta\omega_n t}}{w_d} \sin \omega_d t + d_o \frac{e^{-\zeta\omega_n t}}{w_d} (\omega_d \cos \omega_d t - \zeta\omega_n \sin \omega_d t) \quad (38)$$

$$E[b^2(t)] = \frac{q_2}{4\zeta\omega_n^3} \left[1 - \frac{e^{-2\zeta\omega_n t}}{w_d^2} (\omega_d^2 + 2\zeta\omega_n \omega_d \cos \omega_d t \sin \omega_d t + 2\zeta^2 \omega_n^2 \sin^2 \omega_d t) \right] \quad (39)$$

$$E[d^2(t)] = \frac{q_2}{4\zeta\omega_n} \left[1 - \frac{e^{-2\zeta\omega_n t}}{w_d^2} (\omega_d^2 - 2\zeta\omega_n \omega_d \cos \omega_d t \sin \omega_d t + 2\zeta^2 \omega_n^2 \sin^2 \omega_d t) \right] \quad (40)$$

$$E[b(t)d(t)] = \frac{q_2}{2\omega_d^2} e^{-2\zeta\omega_n t} \sin^2 \omega_d t \quad (41)$$

In the over-damped case, replace sin and cos with sinh and cosh, respectively. In the critically-damped case, let $\omega_d \rightarrow 0$, $\zeta \rightarrow 1$:

$$E[b(t)] = b_o e^{-\omega_n t} (1 + \omega_n t) + d_o t e^{-\omega_n t} \quad (42)$$

$$E[d(t)] = -b_o \omega_n^2 t e^{-\omega_n t} + d_o e^{-\omega_n t} (1 - \omega_n t) \quad (43)$$

$$E[b^2(t)] = \frac{q_2}{4\omega_n^3} [1 - e^{-2\omega_n t} (1 + 2\omega_n t + 2\omega_n^2 t^2)] \quad (44)$$

$$E[d^2(t)] = \frac{q_2}{4\omega_n} [1 - e^{-2\omega_n t} (1 - 2\omega_n t + 2\omega_n^2 t^2)] \quad (45)$$

$$E[b(t)d(t)] = \frac{q_2 t^2}{2} e^{-2\omega_n t} \quad (46)$$

In any case, as $t \rightarrow \infty$,

$$P(t \rightarrow \infty) = \frac{q_2}{4\zeta\omega_n} \begin{bmatrix} 1/\omega_n^2 & 0 \\ 0 & 1 \end{bmatrix}. \quad (47)$$

Thus, the ratio of the steady-state standard deviations of x and \dot{x} will be

$$\frac{\sigma_d}{\sigma_b} = \omega_n, \quad (48)$$

and these are related to the power spectral density by

$$q_2 = 4\zeta \frac{\sigma_d^3}{\sigma_b}. \quad (49)$$